

Special surface for power delivery to wireless micro-electro-mechanical systems

Sylvain Martel

NanoRobotics Laboratory, Department of Computer Engineering and Institute of Biomedical Engineering, École Polytechnique de Montréal (EPM), Campus of the University of Montréal, PO Box 6079, Station Centre-ville, Montréal (Québec), H3C 3A7, Canada

E-mail: sylvain.martel@polymtl.ca

Received 1 November 2004, in final form 4 May 2005

Published 6 September 2005

Online at stacks.iop.org/JMM/15/S251

Abstract

This paper reports a special surface suitable to distribute power while providing a high-precision surface where wireless micro-electro-mechanical systems must operate. The surface is made of alternate electrically conducting and narrower insulating bands with dimensions that allow power to be delivered to the wireless systems when in contact with at least two electrically conductive bands. In this study, a first implementation using stainless steel 440C and black granite is analyzed in more detail. The dimensions of both the conducting and insulating bands are described by considering the properties of the materials used and the precision of the micro-mechanical systems that may be affected by features on the surface with dimensions down to the nanometer scale. The effects on the dimensions of the bands due to the total mass of each microsystem, the contact surface area between the microsystems and the powering surface, and the accuracy of the positioning system used, are also taken into account. Minimum widths of the insulating bands and the methods to prevent electrical shorts between a pair of successive bands, created through arcing between the conductive bands and a conductive structure of the wireless units when stationary or transiting through an insulating band, are also evaluated and compared when operating in air or helium atmosphere.

(Some figures in this article are in colour only in the electronic version)

1. Introduction

In many instances, the level of miniaturization considered for a moving unit such as a micro-electro-mechanical system or a microrobot within the actual technological constraints prevents the implementation of an embedded source of power while a tethered version is not feasible or practical. In [1] for instance, a fleet of scientific instruments in the form of miniature wireless robots ($\sim 32 \text{ mm} \times 32 \text{ mm} \times 30 \text{ mm}$) as depicted in figure 1(a) and designed for interactions at the nanometer scale is described. The level of miniaturization for the design of each robot is a critical factor that increases the density of instruments per platform and hence typically leads to a higher throughput rate of operations while providing more flexibility through independent units to avoid bottlenecks as in the traditional pipeline approach. The real-time functions that must be embedded onto each robot considering the latency

associated when relying on an external computer to perform such tasks at the nanometer scale, result in power consumption per robot exceeding 15–20 watts (W) on average. Because of the insufficient surface on each wireless unit required to dissipate such power while maintaining the temperature of the unit within the operating range without increasing their overall size significantly, these units in the case of the NanoWalker platform are placed in a special cooling chamber where a flow of cooled air or helium (for higher heat conductivity) is used. In such a particular case and in the more general cases based on miniature high-powered wireless units, the PowerFloor must be able to sustain large variations in the temperature levels.

Past experiments have also shown that wired robots based on some types of locomotion, such as the one used for the NanoWalker robot, significantly impede repeatability in motion due mainly to the stiffness and the weight of the wires,

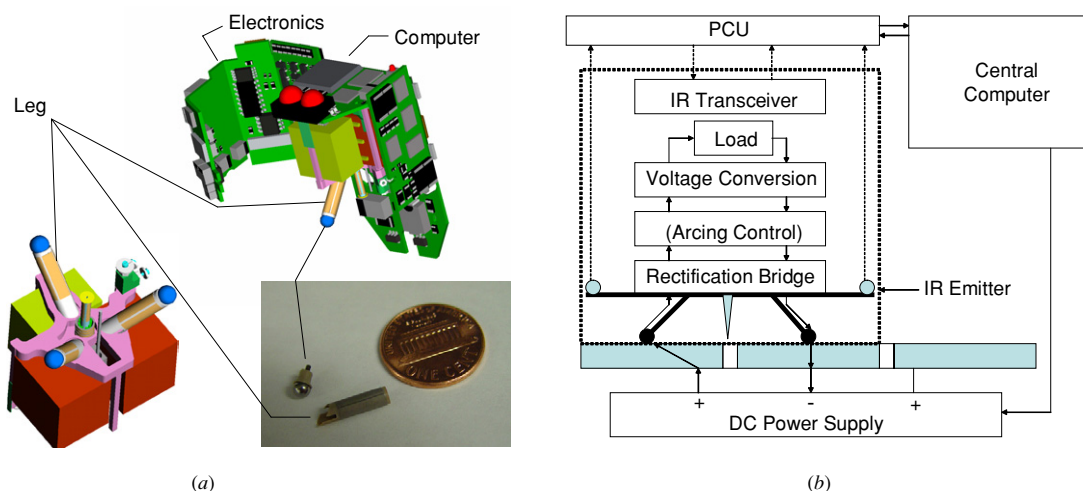


Figure 1. (a) Computer-aided design (CAD) representation of the NanoWalker instrumented robot. It consists of an electronic system in the form of a multilayer flexible circuit (shown unfolded on top of the figure) installed on a three-legged locomotion system (bottom-left) based on piezo-ceramic actuators. The embedded instrument represented here as a STM tip is shown as a tube scanner between the three piezo-legs (bottom-left portion of the figure). A picture of one piezo-ceramic leg with the 'foot' unmounted is shown in the bottom-right portion beside a US penny. (b) Simplified block diagram of the sub-systems involved in the PowerFloor concept. The sub-systems within the dotted box are embedded in the wireless unit whereas the dotted arrows denote wireless links. The arcing control block is required if arcing control is not performed by the central computer.

especially when operating with smaller step sizes down to a few tenths of a nanometer (nm) and/or when the mass of the robot is reduced to increase its mechanical resonant frequency in order to make the unit more suitable at filtering lower frequency vibrations. Furthermore, with a relatively large number of robots sharing the same surface area, the constraints associated with the displacement patterns that would prevent the wires from becoming tangled make such an approach impractical or at least undesirable. To solve these problems, the proposed approach is based on a new concept named 'PowerFloor' and as the name suggests, power delivery is achieved through the floor and the legs of the robots as depicted in figure 1(b).

2. Locomotion system

The locomotion system embedded in each miniature robot consists of three piezo-ceramic actuators in a tubular form and assembled as an equidistant pyramidal shape (120° horizontal, 45° vertical) with the apex pointing upward. Each tube consists of four external electrodes and an inner ground electrode. By applying voltage signals to the quadrant electrodes, bending and stretching in the form of contraction or extension of the legs of the robots can be achieved. A single step is performed by applying voltage signals to each leg to cause the proper vertical and horizontal displacements. Depending on various properties and the overall length of each piezo-leg, the largest steps would typically be in the order of the maximum deflection amplitude of the piezo-tube being approximately $1\text{--}2\ \mu\text{m}$ for a leg with a length of 12 mm but step sizes of $50\ \mu\text{m}$ have been achieved with a lower mass (8 g) prototype version of the NanoWalker robot. The displacement speed is increased with approximately 4000 steps executed per second. Displacements in any direction including rotation are achieved by coordinating and varying the deflections for each leg.

When the legs are in contact with the floor as depicted in figure 1(b), power is transmitted through the legs (with a wire inside the piezo-tube connecting the foot to the embedded electronics) to charge capacitors embedded in the miniature robot. Because the polarity of the voltage levels may change for each leg when a displacement occurs, a rectification bridge is also used. During each step, the contact between the legs and the floor is temporarily lost and the power for the robot then relies entirely on the charge previously stored in the embedded capacitors with a drop in the voltage levels occurring during the discharge. Because the voltage level must be maintained above a minimum value of 6.5 V in this particular implementation to guarantee proper voltage conversions to the remaining embedded electronics, higher dc voltage level on the PowerFloor would allow more time to execute the steps at the cost of increasing power dissipation on each robot and increasing the distance to be considered in the fabrication of the PowerFloor to avoid arcing.

Furthermore, in this particular case, the robot is considered as a scientific instrument designed for interactions and measurements at the nanometer scale, initially through the use of an embedded scanning tunneling microscope (STM). Because of space limitation, the length of the scanning piezo-tube where the STM tip is mounted is also limited and to achieve enough readings per atomic lattice to obtain adequate images within the constraints of the dynamic range and other characteristics (e.g. linearity errors) of the embedded electronics, the scanning range is limited to approximately 200 nm. This suggests that the minimum step sizes achieved by the embedded piezo-locomotion system should be less than 200 nm in order to position the STM tip within an adequate range of a pre-determined position. As such, surface features and flatness of the PowerFloor at such a scale become very important and could be a limiting factor in achieving sufficient accuracy in motion.

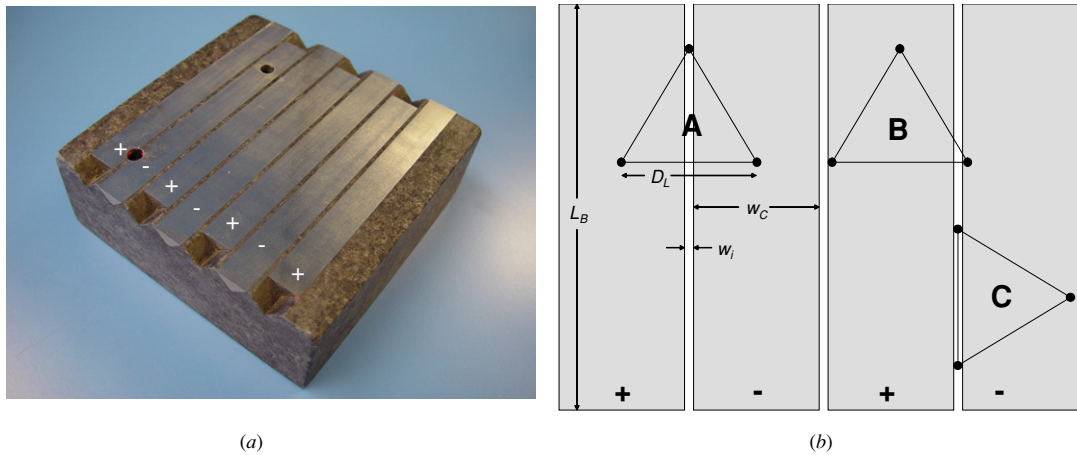


Figure 2. Small version of the PowerFloor designed to accommodate a few miniature robots: (a) implementation of the PowerFloor made of stainless steel 440C for the alternate positive and negative polarity electrically conductive bands mounted on a block of black granite for support and the implementation of the insulating bands, (b) basic diagram of the surface of the PowerFloor. The holes that appear at the surface are receptacles for special atomic grids designed to position each robot at the atomic scale.

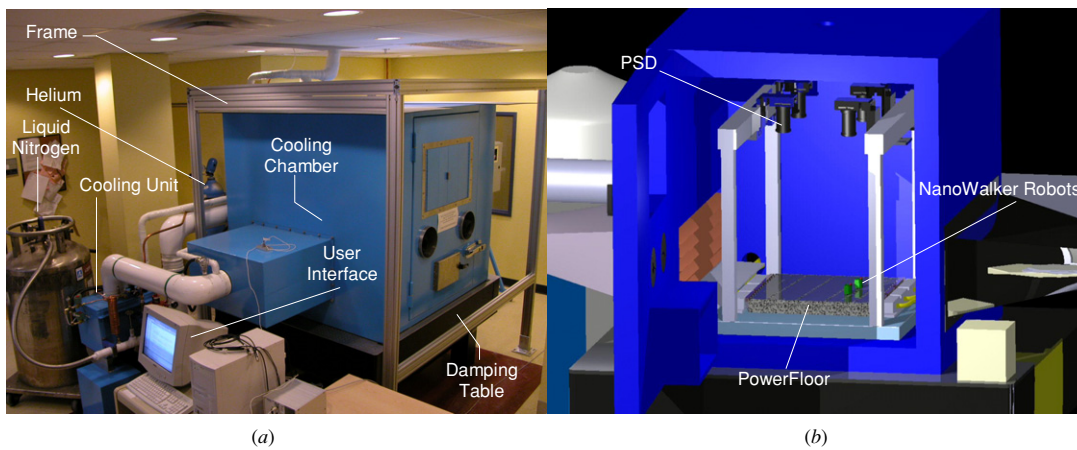


Figure 3. Implementation of the nanorobotics platform designed to accommodate a fleet of at least 100 NanoWalker robots: (a) photograph of the platform with the cooling chamber and (b) showing a CAD representation of the PowerFloor and other main components inside the cooling chamber.

3. PowerFloor

A smaller version of the PowerFloor is depicted in figure 2(a). The final version of the PowerFloor will be larger ($\sim 1.8 \text{ m} \times 1.8 \text{ m}$) than the version shown in figure 2(a) to accommodate a fleet exceeding 100 NanoWalker robots. In principle, the PowerFloor is a simple surface made of alternate power or electrically conductive bands separated by insulating bands. In practice, it can be a relatively complex structure where the parameters such as the coefficient of friction and/or the coefficient of restitution, to name but a few, can have a direct impact on the accuracy of displacement of some types of robots including the NanoWalker robots where such dependence on these parameters was necessary to achieve higher displacement speeds. In general, wireless units including the ones based on the stick-slip method of displacement [2] operating on such a PowerFloor are much less sensitive to these parameters but could be more dependent on the geometry of the surface and the materials being used. Hence in this paper, emphasis is given only to the properties of the materials and the factors

that have an impact on the geometry of both the power and the insulating bands.

A basic diagram of the surface of the PowerFloor is depicted in figure 2(b) showing the positive and negative conductive bands separated by thinner insulating bands. The triangles A, B and C show some possible positions of the intersection between each leg/foot (showed as black dots) for a three-legged robot. In all cases except for triangle C, power can be provided to the miniature robot. To avoid a position such as the one represented by triangle C in figure 2(b) where only one contact point is on a conductive band and referred to here as an idle state, a positioning system is used. In the case of the NanoWalker platform as shown in figure 3(a), a positioning system covering the whole surface area is used. This system, named the global scale positioning (GSP) system (GSPS), is based on four optical position sensing devices (PSD) as depicted in figure 3(b). Each PSD is accompanied by an infrared (IR) communication transceiver and together they form a positioning and communication unit (PCU) (see figure 1(b)). Through an interrogative message sent by

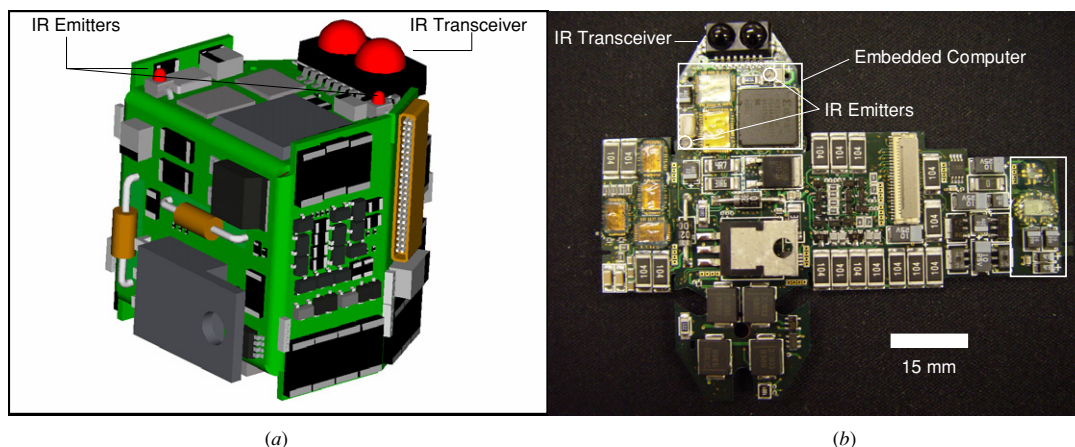


Figure 4. (a) CAD-based representation of the NanoWalker robot showing the IR emitters and IR transceiver on top and (b) a photograph of the upper side (lower side not shown) of the multilayer circuit unfolded showing the position of the IR emitters and IR transceiver.

a central computer to a particular robot through the IR communication link (see figure 1(b)), the robot activates two IR emitters located on top of the robot (see figures 4(a) and (b)), one at a time, to obtain two positions that can be correlated to obtain angular information and hence avoid idle states through corrective actions when moving between two locations.

4. Materials

The materials selected to implement the conductive and the insulating bands are an important issue in the implementation of the PowerFloor. First, because it is easier and less expensive to replace the caps or ‘feet’ of the legs of the robots or micro-electro-mechanical units due to wear over a relatively long period of operation, the hardness (often specified in Rockwell C (HRC) or Mohs and being an indication of the material’s resistance to surface damage which would affect the motion accuracy of the wireless unit) of the materials chosen to implement the conductive and insulating bands is typically higher than the hardness of the material selected to implement the caps of the legs. Although many materials could have been selected, for practical reasons such as availability and ease of fabrication, initially stainless steel AISI type 302 (HRC: 25–39 (non-annealed), Poisson ratio: 0.27–0.30 GPa @ 25 °C, elastic modulus: 193 GPa @ 25 °C) [3] or stainless steel AISI type 404 (HRC: 35, Poisson ratio: 0.27–0.30 GPa @ 25 °C, elastic modulus: 190–210 GPa @ 25 °C) have been considered. The AISI 300 series are austenitic iron–chromium–nickel alloys whereas the AISI 400 series are ferritic and martensitic alloys. Stainless steel 302, for instance, is available commercially in the form of ball bearings which is very convenient for capping the legs in terms of ease of fabrication, alignment and replacement. It is also non-magnetic and has a high toughness at all temperatures, which is an important factor especially when operating in a cooling chamber. Stainless steel 302 is made of a maximum of 0.15% carbon, 2.00% manganese, 0.045% phosphorus, 0.030% sulfur, 1.00% silicon, 17.00–19.00% chromium, 8.00–10.00% nickel, 0.10% nitrogen and 3.00–4.00% copper (type HQ). High oxidation-resistance in air at ambient temperature is normally achieved with the addition

of more than 12% (weight) chromium. The ratio of 17–19% chromium for the stainless steel AISI type 302 compared to the ratio of 11.0–12.5% for the AISI type 404 favors the choice of the AISI type 302 over 404 (which is still an interesting option and which has similar characteristics) for units such as the NanoWalker robots that are based on precise locomotion mechanisms that are affected by changes in friction coefficient due to oxidation.

Stainless steel AISI type 440C (HRC: 58–65 (5 Mohs) (treated), Poisson ratio: 0.27–0.30 GPa @ 25 °C, elastic modulus: 200 GPa @ 25 °C) to implement the conductive bands and black granite (5–7 Mohs, Poisson ratio: 0.20–0.30 GPa (compression) @ 25 °C, elastic modulus: 40–70 GPa @ 25 °C) for the insulating bands have been selected initially. Stainless steel 440C has a higher toughness than stainless steel 302. It also has very good oxidation-resistance properties (it contains 16–18% chromium) improving with a higher polish at the surface, which may result in a noticeable impact on the coefficient of friction and hence, the motion behavior of the robots. Stainless steel AISI type 440C is made of 0.95–1.20% carbon, 16.0–18.0% chromium, 1.00% silicon, a maximum of 1.0% manganese, 0.040% phosphorous, 0.030% sulfur and 0.075% molybdenum. The electrical resistivity (specified at 25 °C) of stainless steel 440C at $600 \times 10^{-9} \Omega \text{ m}$ is also approximately the same as stainless steel 302 specified at $720 \times 10^{-9} \Omega \text{ m}$. On the other hand, the properties of the black granite surface should approach the ones for stainless steel 440C. Black granite has a high modulus of elasticity, tight porosity and very fine grain. Since it contains no crystalline quartz, its wear life is less than that of crystal pink granite surface. However, black granite has a very fine finish and meets flatness requirements equally well but may need relapping more often than crystal pink granite. Black granite is generally accepted as the best because of its lower porosity and moisture absorption, superior strength and lower coefficient of thermal expansion being particularly important in the changing temperature environment of the proposed platform. The superior ‘stiffness’ of black granite is also highly desirable here where accuracy and stability are essential.

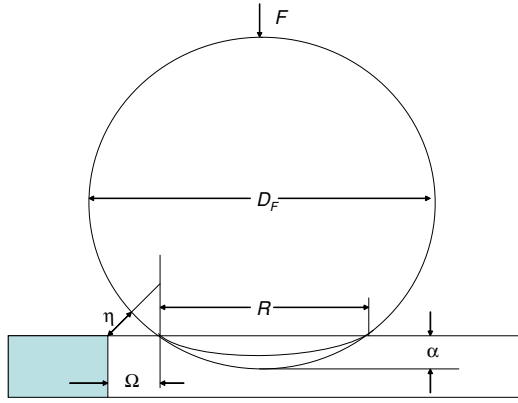


Figure 5. Basic model of the extremity of a leg (foot) on the insulating band of the PowerFloor. The shadowed region represents a conductive band. F , R , η and α represent the force acting on the foot, the chord of the surface contact, the minimum distance to prevent arcing and the elastic compression, respectively.

5. Nanometric characteristics

The PowerFloor is an accurate structure but its specifications under various conditions must be known and controlled within acceptable limits especially when used as a part of a microfactory or a nanofactory where its characteristics at the nanometer level must be known. A first issue is to minimize non-conductive area and crossovers between the conductive and the insulating bands in order to facilitate the avoidance of idle states. As such, the width of each conductive band w_c is made as large as possible but the condition ($w_c + w_i < D_L$), where w_i is the width of the insulating band and D_L is the distance between two legs in an equidistant configuration as depicted in figure 1(a) at the contact point between the legs (feet) and the floor, must be met. On the other hand, w_i should be as narrow as possible but larger than a specific width ($\min w_i$). This minimum width depends mainly on the surface contact cross section or chord (denoted as R in figure 5), thermal expansion, the angular accuracy of the positioning system (the GPS for the NanoWalker platform) and possibly the minimum distance (denoted η in figure 5) required to prevent arcing which also depends on the dielectric of the

atmosphere surrounding the foot or contact structure of the wireless unit.

In order to avoid electrical shorts between a successive pair of negative and positive conducting bands through arcing with the spherical foot in this particular case, we must have

$$w_i > R + 2\Omega. \quad (1)$$

In equation (1), Ω as depicted in the diagram in figure 5 depends not only upon the value of η but also on the value of R . By considering these materials, a first estimation of ($\min w_i$) through a calculation of the elastic compression between the caps of the legs and the floor can be done. In the general case, the total elastic compression α at the point or line of contact between a sphere with diameter D_F and representing the ‘foot’ of each leg with a plane or floor measured along the line of the applied force F or normal contact pressure can be computed as

$$\alpha = \frac{(3\pi)^{2/3}}{2} \cdot F^{2/3} \cdot (v_1 + v_2)^{2/3} \cdot \left(\frac{1}{D_F}\right)^{1/3}, \quad (2)$$

$$v = \frac{(1 - \sigma^2)}{\pi E}. \quad (3)$$

In equation (3), σ and E represent the Poisson ratio and Young’s modulus of the material of the body respectively. Figure 6 shows the estimated elastic compression caused by a single leg capped with a 3.0, 1.0 and 0.1 mm diameter ball made of stainless steel 302 or 404 on a granite surface for a three-legged robot with a total mass ranging from 15 g to 100 g as expected on the final implementation of the robot and based on initial designs. Young’s moduli of 193 and 40 GPa with Poisson ratios of 0.27 and 0.20 have been considered for worst-case analysis for the ball and the granite surface, respectively.

One possible method to reduce ($\min w_i$) is to reduce D_F at the cost of increasing the elastic compression as depicted in figure 6 where the normal force is assumed to be the same at each leg. This method is limited by the elastic limit (causing permanent or plastic deformations or damage) between the foot and the surface (yield strength). From these values, the line segment or chord R can be estimated (equation (4)) as

$$R = 2 \cdot \sqrt{\left(\frac{D_F}{2}\right)^2 - \left(\frac{D_F}{2} - \alpha\right)^2}. \quad (4)$$

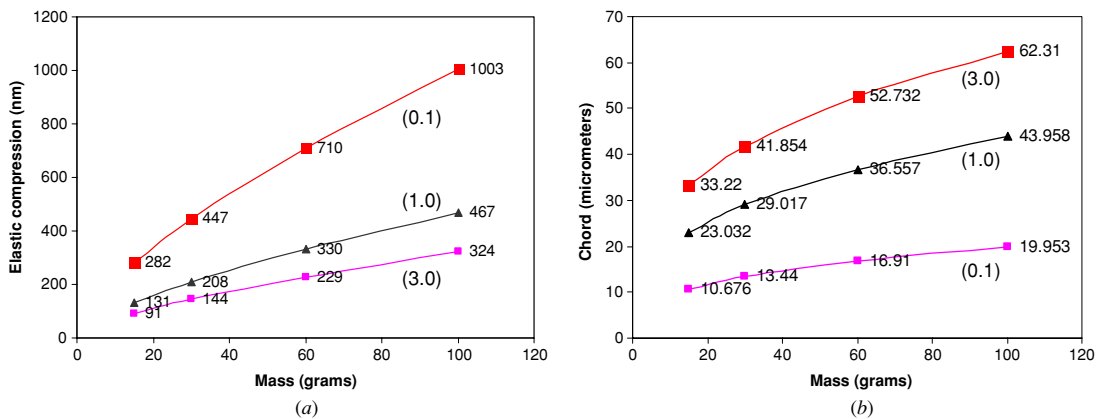


Figure 6. (a) Estimation of the elastic compression versus the total mass of the three-legged robot at 25 °C between a single leg and the insulating band with $D_F = 3.0, 1.0$ and 0.1 mm and (b) resulting chord length R . The results assume a perfectly flat surface.

The results are plotted in figure 6(b) with a total mass of the robot varying between 15 and 100 g and assuming a precise diameter D_F . The value of R may impact sensibly on the motion behavior of the wireless unit depending on the method of displacement but more importantly, it defines a cross-sectional contact area between a ‘foot’ and the PowerFloor that lowers the electrical resistivity of the conducting channel as R increases within a limit determined by the locomotion system. Fortunately, lowering the environmental temperature in the chamber to cool the wireless units also contributes to lower such resistivity.

The arcing distances can typically be derived from Paschen’s law but deviations from these previous studies have been observed for gaps below $10 \mu\text{m}$ [4]. In [5], the smallest potential difference measured in air ($\sim 1 \text{ Atm}$) was 12 V at $0.25 \mu\text{m}$. Since the maximum dc voltage level of the positive bands of the actual PowerFloor of the NanoWalker platform can vary from 6.5 V to 12 V depending on the types of operations (assuming 0 V for the negative bands), η can be estimated at $0.25 \mu\text{m}$ in the worst case when operating in air. Since the dielectric strength or breakdown voltages of air and helium are 0.97 and 0.15 respectively (nitrogen = 1.00), η can be estimated at $1.62 \mu\text{m}$ in the worst case when operating in helium.

From these results, the values of $(\min w_i)$ can be computed easily from equation (1) within an air or helium atmosphere with Ω estimated by simple geometry. But practically, the width of the insulating bands must be extended to deal with the tolerance in the assembly process of the locomotion system, the additional gaps between the stainless steel bars and the granite to compensate for thermal expansions (because such gaps are electrically non-conductive they are assumed to be parts of the insulating bands), and possibly enlarged if the angular precision of the global positioning system is not sufficient (which will be reduced with a reduction of the micro-mechanical systems due to a decrease in the distance between the two IR emitters on the same wireless unit). Furthermore, the results may be influenced by the flatness of the surface.

6. Arcing control

Even if the condition expressed in equation (1) is met, erosion of the structures (feet and conducting bands) could occur when a foot approaches a conducting band from an insulating band. There are two main approaches to avoid this problem, referred to here as embedded arcing control (EAC) and centralized arcing control (CAC). With the EAC, a special circuit embedded in each wireless unit (see figure 1(b)) is activated to provide high impedance to the power input of a particular leg or another structure in contact with the PowerFloor. To avoid the added complexity for the embedded electronics, the CAC executed in the central computer will switch on or off the power to eliminate the difference in potentials to a respective power tile based on the position of the wireless unit (see figure 1(b)). Power or conducting tiles here are typically squared regions within a conductive band where the power applied can be controlled individually and has the potential to decrease the required value for Ω at the cost of added complexity in the implementation of the PowerFloor.

7. Method of encapsulation

The method of encapsulation of the conducting bands onto the insulated granite block was performed as follows: (1) the granite block was ground to the desired shape and the chamfers were done, (2) a precision grinding process of the granite block to the specified quality (lab AA) followed, (3) the V shape grooves and placement holes were machined, (4) the 440C bars were ground down to specifications, (5) the 440C V-shaped bars were adhered in place with an epoxy and (6) the whole assembly was ground down to the desired dimensions and specifications.

A gap of a few micrometers was implemented between each stainless steel 440C and the granite. The width of the gap was maintained to a minimum to minimize the error amplitudes for the motion of the wireless units when transiting through the gap and to minimize the additional force that may be required by the locomotion system to transit through such gaps. On the other hand, the width of the gap must be sufficient to compensate for the thermal expansion of the material used for the PowerFloor within the range of ambient temperatures used, within the cooling chamber in this particular case.

8. Results and discussion

For the PowerFloor depicted in figure 2(a), even if the stainless steel bars and the granite were ground down simultaneously, measurements of the surface by a profilometer depicted in figure 7 indicate differences in flatness between the stainless steel 440C and the granite with average Ra of $0.08 \mu\text{m}$ and $0.88 \mu\text{m}$, respectively, indicating a better flatness for the conducting bands. Furthermore, the values of Ra were not constants in all directions, suggesting that the grinding process should be done following linear paths instead of rotational paths. Experiments showed that the grinding process affects the displacements of the NanoWalker robot.

The differences in flatness between the conducting and insulating bands are major. For the stainless steel, the variation in surface flatness is in the order of a few hundred nanometers compared to a few micrometers for granite as depicted in figures 7(a) and (b), respectively. The difference between the conducting and insulating bands is also visible in figure 7(c) with larger variations observed over an insulation band of the experimental PowerFloor, depicted in figure 2(a), of 2.2 mm width. These results suggest that corrective actions would be necessary when a leg transits across one of these insulation bands. The results also indicate that although corrective actions can be considered when transiting between two working locations, all three legs should be in contact with the conducting bands even if only two legs are necessary to provide electrical power, when performing final accurate displacements to position the STM tip in order to avoid additional errors due to the higher variations in flatness of the insulation bands. Furthermore, it appears from figure 7(a) that the magnitude of variations in the flatness of the conducting bands is already large compared to the elastic compression values (figure 6(a)) that may affect the accuracy in displacement especially for micro-mechanical systems with a lower mass.

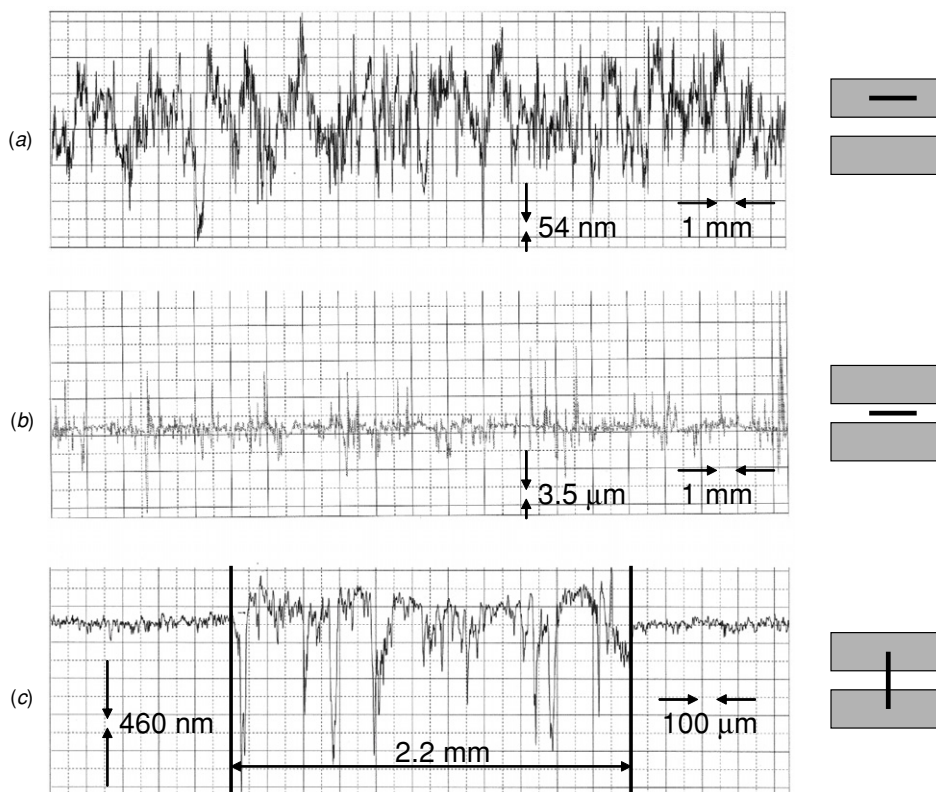


Figure 7. Flatness of the surface of the PowerFloor measured with a profilometer: (a) along the longitudinal axis of a 440C stainless steel conducting band, (b) along the longitudinal axis of a back granite insulation band and (c) along the transversal axis between two conducting bands.

The width of 2.2 mm of the insulation bands here was determined somewhat arbitrarily. For instance, if we consider a worst-case scenario for various designs of the NanoWalker robot with a total weight of 100 g and feet with diameter of 3 mm and operating in helium, a minimum width of the insulating bands estimated at approximately $65 \mu\text{m}$ could be sufficient. To this value, we must add small gaps of a few micrometers in the worst case between the insulating and powering bands to compensate for thermal expansions. The tolerance or errors in the assembly of the robots for the actual distance between the IR emitters used for positioning (see figure 1(b)) and the actual locations of the legs at the contact point with the floor will also increase the value of the minimum width required. The variation or tolerance in the fabrication of the PowerFloor is also another factor to consider. Finally, errors related to the locomotion and the positioning system also affect the total minimum width of the insulation bands required. Since the PowerFloor depicted in figure 2(a) was developed to conduct initial experiments, an excessive width of 2.2 mm was selected initially to reduce the constraints on the various experiments. In the final implementation, this width would be minimized to offer the largest percentage of homogeneous surface and to minimize the constraints in angular orientation of the robots during transits and at the final working site. It is also important to maintain the gap for thermal expansion as small as possible and to ensure that it is smaller than the maximum step sizes of the robots.

9. Conclusion

A new approach for powering wireless units within platforms such as micro-/nanofactories has been briefly described. The method based on a new concept called 'PowerFloor' requires special attention and a good understanding of its characteristics at a scale that is dependent not only on the working environment but also on the scale that such units must operate. Hence, a nanometer-scale analysis would become essential when implemented in the context of a nanofactory or a platform with instruments in the form of microrobots capable of interacting at the nanometer scale. As such, parameters such as thermal expansion, flatness, conductivity, resistance to oxidation, overall size of the micro-mechanical systems and in particular the position of the actuators and its weight, tolerances and errors related to assembly and positioning, locomotion mechanisms and many characteristics of the materials used such as Poisson ratio and Young's modulus, to name but a few, must be taken into account when designing such PowerFloor especially for operations requiring higher accuracy.

Acknowledgments

The author acknowledges the kind support of Neila Kaou and Kwang Soo Kim for assisting in the verification of some aspects of this paper. The project is presently funded in part by a Canada Research Chair (CRC) in conception, fabrication and validation of micro/nanosystems and grants

from the National Sciences and Engineering Research Council of Canada (NSERC), Valorisation Recherche Québec (VRQ) and the Canada Foundation for Innovation (CFI).

References

- [1] Martel S and Hunter I 2004 Nanofactories based on a fleet of scientific instruments configured as miniature autonomous robots *J. Micromechatronics* **2** 201–14
- [2] Breguet J M, Permette E and Clavel R 1996 Stick and slip actuators and parallel architectures dedicated to microrobotics *Proc. SPIE* **2906** 13–24
- [3] http://www.efunda.com/materials/alloys/stainless_steels/stainless.cfm
- [4] Meek J M and Craggs J D 1953 *Electrical Breakdown of Gases* (Oxford: Oxford University Press)
- [5] Dhariwal R S, Torres J M and Desmulliez M P Y 2000 Electric field breakdown at micrometre separations in air and nitrogen at atmospheric pressure *IEE Proc. Sci. Meas. Technol.* **147** 261–5